Analysis of Cake Filtration Data—A Critical Assessment of Conventional Filtration Theory

Soo-Khean Teoh, R. B. H. Tan, and Chi Tien
Dept. of Chemical and Biomolecular Engineering, National University of Singapore, Singapore, 119260

DOI 10.1002/aic.10952
Published online August 8, 2006 in Wiley InterScience (www.interscience.wiley.com).

Experimental results of constant-pressure cake filtration of aqueous suspensions of four kinds of particles: $CaCO_3$, Kaolin, Kromasil and TiO_2 is presented. The data reported consist mainly of filtration performance results, that is, the cumulative filtrate volume and cake thickness as functions of time, which were obtained using a newly developed multifunction test cell. Based on these data, the medium resistance and the average cake specific resistance at various operating pressure were evaluated and corroborated with the results obtained from the compression-permeability (C-P) cell measurements. The filtration results were also compared with predictions from the solutions of the appropriate volume-averaged equations of continuity using different $p_l - p_s$ relationships. Generally speaking, with the appropriate $p_l - p_s$ relationship, agreement between experiments and prediction was satisfactory. © 2006 American Institute of Chemical Engineers
AIChE J, 52: 3427–3442, 2006
Keywords: cake filtration, specific cake resistance, medium resistance, filtration performance, filtration data

Introduction

As a subject of study, experimental investigation of cake filtration has received considerable attention in the past because of the importance of cake filtration as a method for solid/liquid separation. Beginning with the work of Ruth,[1,2] a large number of investigations mainly those by Grace,[3,4] Tiller and coworkers,[5–18] and Shirato and coworkers,[19–24] have appeared in the literature. These studies were concerned mainly with the confirmations and descriptions of the dynamics of filtration; determinations of filter cake characteristics, as well as the effect of certain complicating factors, such as sedimentation encountered in cake filtration.

In spite of the large number of studies made in the past, certain problems remain unresolved (for example, the correspondence between the C-P cell measurement results and those obtained directly from filtration experiments). More importantly, recent studies on cake filtration analysis yield results, the confirmation and validation of which require data not given in these previous studies. It is for these reasons that the present study was undertaken.

The purpose of the present study is to conduct constant-pressure filtration experiments using suspensions of different kinds and carry out compression-permeability measurements of these systems. The experiments and measurements were conducted using a newly developed multifunction test cell which may function as a filtration vessel, and also as a compression-permeability (C-P) cell. This dual-function feature makes it possible to compare C-P cell measurement results with filtration data in a more unequivocal manner. The specific objectives of the study are:

1. To examine the effect of the relationship between the liquid pressure and cake compressive stress in predicting filtration performance.
2. To provide data for comparisons of filtration performance (namely, the histories of the cumulative filtrate volume and cake thickness) with predictions based on the solution of the appropriate volume-averaged equations of continuity.
3. To compare the initial period of filtration results with the analysis of Koenders and Wakeman.[25–27]

Correspondence concerning this article should be addressed to R. B. Tan at reginald@nus.edu.sg.
Current Address: Dept. of Chemical Engineering and Materials Science, Syracuse University, Syracuse, NY.

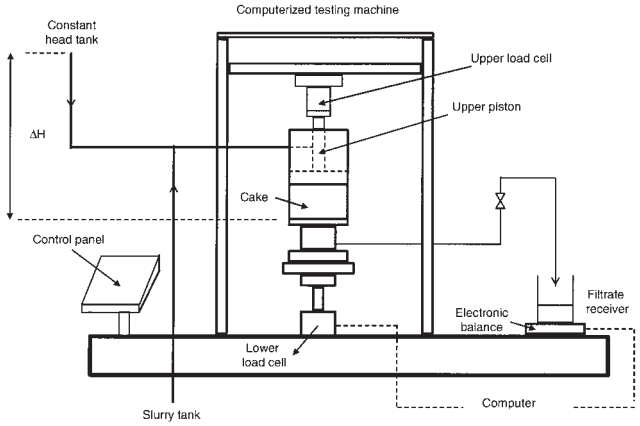

Figure 1. Multifunction test cell.

4. To determine the variations of the medium resistance with the applied pressure.

Experimental

Apparatus

The apparatus used in this study is shown in Figure 1. The main apparatus is a multifunction cell recently developed at the National University of Singapore, which can be used for both filtration experiments and compression-permeability (C-P) measurements. The test cell was fabricated by modifying a commercial computer-controlled universal testing machine (Shimadzu Autograph AGS-10kNG) commonly used for determining the mechanical strength of materials. The cell consists of an upper piston through which a constant applied loading may be applied and a complimentary lower piston. Test suspension enters into the cell through a central pore of the upper piston, and filtrate leaves the cell through a bore of the lower piston. The cell has a height of 9.5 cm, and an inner diameter of 7.5 cm. When used for filtration experiments, the cell is configured by fitting an interchangeable insert plate with a sharp orifice to the bottom of the upper piston. The insert plate has a raised cylindrical portion surrounding the orifice opening such that when the insert plate is in place, the distributor portion of the upper piston is closed off; thus, restricting the flow of the test suspension through the orifice only. This design was made following the work of Murase et al.[28] and detailed features of the test cell are shown in Figure 2. More complete descriptions of the cell can be found elsewhere,[29–31] and will not be repeated here.

Materials

Aqueous suspensions of $CaCO_3$, Kaolin, TiO_2 and Kromasil powders were used in the experimental work. The relevant properties of these powders and their sources of supply are given in Table 1.

For filtration experiments, test suspensions were prepared by mixing specific amounts of test powder of a given type with

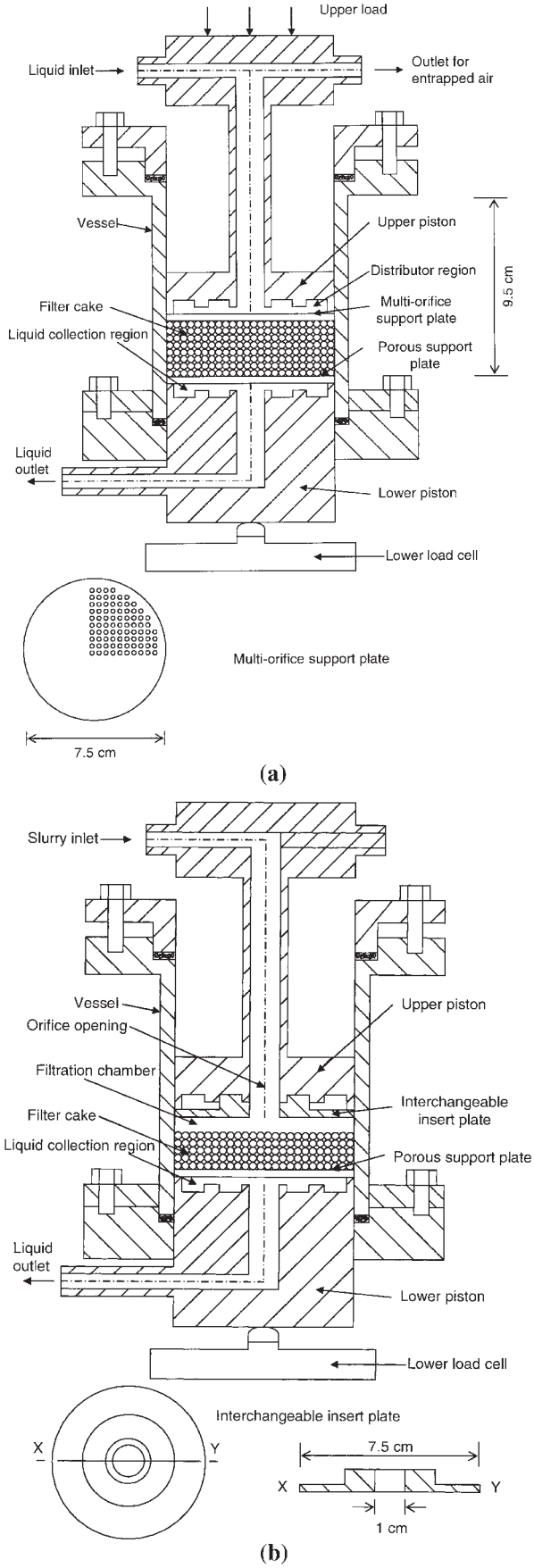

Figure 2. Features of the multifunction test cell.

(a) As a compression-permeability cell and (b) as a filtration cell.

Table 1. Properties of Test Particles

System	$CaCO_3$	Kaolin	TiO_2	Kromasil
Particle Density, ρ_s (kg m^{-3})	2655	2704	3867	2005
Moisture Content, (% at 23°C, RH 75%)	0.36	0.78	0.39	3.43
Mean Particle Size, (μm) (volume based)	3.847	9.043	0.39	3.43
Source of Supply	Fisher Scientific	Merck	Univ. of Magdeburg (Germany)	Univ. of Magdeburg (Germany)

deionized water. The mixture was then stirred at 25 rpm for at least 1/2 h prior to its use.

Procedures

Two types of measurements, constant pressure filtration and compression-permeability measurement were made in this work. The procedure used to conduct these measurements is described as follows.

For constant-pressure filtration experiments, before each experiment, a number of Whatman No. 1 filter paper, constituting the filter medium (septum) were placed on the support plate of the lower piston. The position of the upper piston was fixed, thereby, enclosing between it and the lower piston a chamber of fixed volume. Test suspension of known concentration was introduced into the chamber by means of compressed nitrogen gas. During each experiment, the filtrate collected was recorded on line. The thickness of the cake formed increased with time. When the cake reached the upper piston, a sharp decrease in filtration rate occurred. Thus, from the time history of cumulative filtrate volume, the time when the filter cake thickness reached a particular value corresponding to the position of the insert plate was determined. This will be further discussed later.

The C-P measurements were made in order to obtain the relationships between cake solidosity, ε_s (and permeability, k and, therefore, the specific cake resistance, α) and the compressive stress to which the cake was subject.

The procedure used to conduct the C-P measurement was the same as that used by the authors previously.[30] Briefly speaking, before each measurement, sheets of wetted filter paper were placed below the multiorifice plate of the upper piston, and on the support plate of the lower piston. A slurry prepared with a known mass of test powders (50 grams of $CaCO_3$, 100 grams of Kaolin, 60 grams of TiO_2 and 40 grams of Kromasil) and sufficient amount of deionized water was poured carefully into the cell, and by settling, a filter cake of loose packing was formed over the lower piston. The upper piston was then lowered into the cell to compress the preformed cake at a specified loading. The downward vertical movement of the upper piston was recorded as a function of time, as well as the load transmitted to the lower piston (measured by the load cell). This process continued for about 24 h until the cake reached its mechanical equilibrium, as shown by the attainment of a constant cake thickness.

Upon the formation of the cake, deionized water under a specified pressure entered into the cell through the liquid inlet of the upper piston and passed through the cake. The flow of the deionized water was determined for the liquid collected (as measured by an electronic balance). The flow rate-pressure drop data were then used to determine the cake permeability.

Results

Compression-permeability measurements

These measurements yield results of the following types; cake thickness, transmitted compressive force vs. compressive force applied for cake formation and the pressure drop-flow rate data for the cake formed. From cake thickness, the cake solidosity is found to be

$$\varepsilon_s = \frac{m}{LA\rho_s} \tag{1.a}$$

where m is the mass of the test powder used to form the cake, ρ_s the powder density, L the cake thickness, and A, the cross sectional area of the cell.

Table 2. Compression-Permeability Measurement Results of ε_s, k and α vs. p_s

System	p_s (Pa) 1×10^5	ε_s (—)	α (m kg^{-1}) 1×10^{11}	k (m^2) 1 $\times 10^{-15}$
$CaCO_3$ Cake	0.405	0.228	0.521	31.7
	0.916	0.228	0.610	27.2
	1.34	0.225	0.713	23.5
	2.69	0.239	0.867	18.2
	3.61	0.255	1.02	14.6
	4.56	0.251	1.12	13.4
	5.47	0.255	1.27	11.6
	6.41	0.285	1.21	10.9
	7.28	0.291	1.32	9.83
	8.27	0.298	1.41	8.94
Kaolin Cake	0.881	0.377	9.83	0.999
	1.75	0.410	13.9	0.651
	2.72	0.427	19.6	0.442
	3.64	0.439	20.8	0.406
	5.49	0.465	30.7	0.259
	6.40	0.467	32.6	0.243
	7.35	0.497	37.7	0.197
	8.29	0.503	40.5	0.182
TiO_2 Cake	7.68	0.337	7.59	1.01
	1.71	0.379	10.3	0.660
	2.62	0.404	9.23	0.693
	3.52	0.411	11.8	0.533
	4.40	0.423	14.3	0.428
	5.33	0.438	15.7	0.377
	6.30	0.447	15.8	0.367
	8.02	0.455	17.0	0.334
Kromasil Cake	7.82	0.242	0.549	37.6
	1.70	0.246	0.714	28.4
	3.51	0.251	0.814	24.4
	4.46	0.251	0.732	27.1
	6.33	0.256	0.109	17.9
	7.22	0.258	0.114	16.9
	8.14	0.258	0.107	18.1

Table 3. Constitutive Parameters of $CaCO_3$, TiO_2, Kaolin and Kromasil Cake Determined from C-P Measurements

Quantity	$CaCO_3$	Kaolin	TiO_2	Kromasil
ε_s^o (—)	0.20	0.34	0.31	0.21
k^o (m^2)	4.8915×10^{-14}	1.9885×10^{-15}	1.4817×10^{-15}	1.8411×10^{-13}
α^o (m Kg^{-1})	3.85×10^{10}	5.47×10^{11}	5.63×10^{11}	1.29×10^{10}
β (−)	0.13	0.17	0.17	0.03
η (−)	0.57	1.02	0.68	0.35
n (−)	0.44	0.85	0.51	0.32
Pa (Pa)	4.4×10^4	8.7×10^4	9.9×10^4	1.0×10^3

Table 4. Conditions of Constant-Pressure Filtration Experiments

	Suspension			
Variable	$CaCO_3$	Kaolin	TiO_2	Kromasil
Applied Pressure, p_o (Pa) 1×10^5	1.0–7.7	0.9–8.0	1.0–8.0	0.9–7.8
Particle Density, ρ_s (kg m^{-3})	2,655	2,704	2,704	2,005
Mass Fraction of Suspended Particles, s (kg kg^{-1})	0.02	0.05	0.02	0.02
pH of Suspension	10.6	6.8	7.1	6.0

The cake permeability was determined according to Darcy's law, or

$$k = \frac{Q}{A}\frac{\mu L}{\Delta p} \tag{1.b}$$

where Q is the volumetric flow rate, μ, the liquid viscosity and Δp the pressure drop across the cake.

To obtain the results of ε_s (or k) vs. p_s, p_s was estimated to be[32]

$$p_s = \left(\frac{1}{A}\right)\frac{F_A - F_T}{\ell n \dfrac{F_A}{F_T}} \tag{2}$$

where F_A and F_T are the applied and transmitted force, respectively.

The results of ε_s, k and α vs. p_s are listed in Table 2. According to the common practice, these data can be fitted by the power law expression, or

$$\varepsilon_s = \varepsilon_s^o\left(1 + \frac{p_s}{p_a}\right)^{\beta} \tag{3}$$

$$k = k^o\left(1 + \frac{p_s}{p_a}\right)^{-\eta} \tag{4}$$

$$\alpha = \alpha^o\left(1 + \frac{p_s}{p_a}\right)^{n} \tag{5}$$

where ε_s^o, k^o, α^o,* β, η, n and p_a, are empirical constants. From the definition of α, one has

$$\alpha^o = (\varepsilon_s^o k^o p_s)^{-1} \tag{6}$$

$$n = -\beta + \eta \tag{7}$$

The values of the parameters are given in Table 3.

Constant-pressure filtration experiments

These experiments were conducted using the four types of suspensions described before. The data obtained includes the cumulative filtrate volume and cake thickness as functions of time. The variables considered were the applied pressure, the suspension particle concentration, the particle size and density, the medium resistance, and the position of the upper piston (for the determination of cake thickness vs. time). The experimental conditions used are summarized in Table 4.

As stated before, the method used for determining the cake thickness vs. time was based on the method first proposed by Murase et al.[28] For each filtration experiment, the upper piston of the test cell was placed at a particular position. The test suspension entered into the cell through the inlet opening of the piston. Initially there was sufficient space between the upper piston, and the surface of the cake formed so that the entering suspension was distributed evenly over the cross section of the cell before it reached the cake/suspension interface. As the cake thickness approached the cell height, suspension distribution was hindered and the reduction of the effective filtration area led to a reduction of the filtration rate. This change of the filtration behavior can be seen through a plot of t/v vs. v (see Figure 3). As shown in the figure, the data can be represented by two linear segments. The intersection of these two-linear segments gives the time when the cake thickness equals the cell height.

The results of the cake thickness vs. time for the cases of $CaCO_3$ and Kaolin suspensions are given in Table 5.

A typical set of the cumulative filtrate volume vs. time data is shown in Figure 4. The data shown in the figure were obtained from the experiments of 2% $CaCO_3$ suspension with filter medium composed of a number of Whatman No. 1 filter papers. The discussion to be given in the following section will be largely based upon these data.

* ε_s^o, k^o and α^o can also be considered as the values of ε_s, k and α at the zero-stress state.

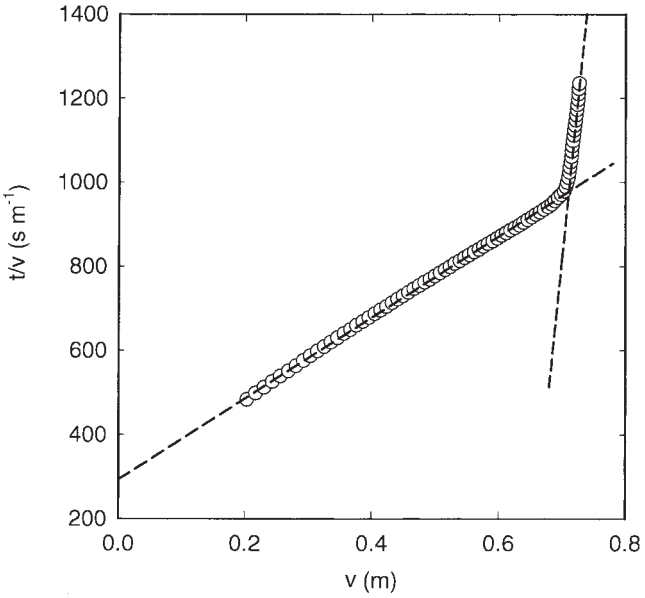

Figure 3. Determination of the relationship of *L* vs. *t* according to the procedure of Murase et al.[28]

v vs. t Data obtained under the condition p_o = 800 kPa, 2% $CaCO_3$ suspension. Preset cake height 20 mm, two whatman No. 1 filter paper as medium.

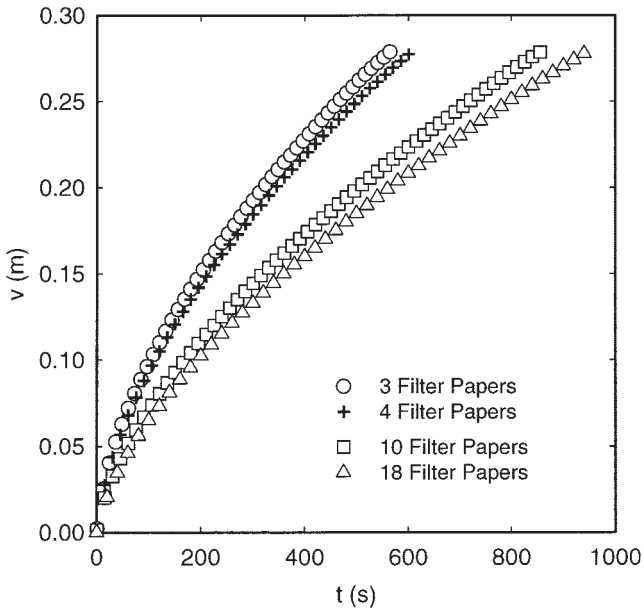

Figure 4. Effect of medium resistance on constant-pressure filtration performance. Filtration of 2% $CaCO_3$ at p_o = 100 kPa.

Medium composed of a fixed number of whatman No. 1 filter paper.

Discussion

Background information

The background information used in interpreting and discussing the experimental results will be first reviewed.

1. Constant-Pressure Filtration According to the Conventional Filtration Theory. The most commonly used method of interpreting constant-pressure cake filtration is based on the so-called parabolic law. With the assumption that the pressure drop across the cake is essentially the same as the applied pressure (namely, the medium resistance is negligible), the wet to dry cake mass ratio is constant, and the particle velocity within the cake is small as compared with the filtrate velocity, the relationship between the cumulative filtrate volume per unit filtration area, v and time t, is

$$p_o t = \frac{\mu \rho s (\alpha_{av})_{p_{s_m}}}{2(1 - \bar{m}s)} v^2 + \mu R_m v \tag{8}$$

Table 5. Results of Cake Thickness vs. Time at Various Applied Pressure for Constant Pressure Experiments

System: $CaCO_3$	p_o = 100 kPa	p_o = 500 kPa	p_o = 800 kPa
L (m)	t (s)	t (s)	t (s)
0.01	1200	380	320
0.02	3160	1040	730
0.03	6650	2270	1760
0.04	11370	3210	2440
0.05	16860	5620	4100
System: Kaolin	p_o = 100 kPa	p_o = 500 kPa	p_o = 800 kPa
L (m)	t (s)	t (s)	t (s)
0.005	2330	1420	1270
0.010	7540	6050	5130
0.015	22080	14400	12120
0.020	38320	24270	20970

where p_o is the applied pressure, s, the particle mass fraction of the suspension to be filtered; ρ, the filtrate density, $\bar{m}$, the average wet to dry cake mass ratio, μ, the filtrate viscosity, and R_m, the medium resistance. $(\alpha_{av})_{p_o}$ is the average specific cake resistance for $0 < p_s < p_{s_m}$ and is defined as

$$(\alpha_{av})_{p_{s_m}} = \frac{p_o / p_{s_m}}{\left[\int_o^{p_{s_m}} \left(\frac{1}{\alpha}\right)(-f')dp_s\right] \Big/ p_{s_m}} \tag{9}$$

and

$$f' = \frac{dp_\ell}{dp_s} \tag{10}$$

$$\int_o^{p_{s_m}} (-f')dp_s = p_o \tag{11}$$

where p_ℓ and p_s are the liquid pressure and cake compressive stress, respectively. If $f' = -1$, the earlier set of equations becomes one which is commonly used in filtration data interpretation. Derivations of these equations can be found in the work of Tien et al.[33] and Tien and Bai.[34]

Equation 8 can be rearranged to give

$$\frac{t}{v} = \frac{\mu \rho s (\alpha_{av})_{p_{s_m}}}{2(1 - \bar{m}s)p_o} + \frac{\mu R_m}{p_o} \tag{12}$$

According to Equation 12, a plot of v vs. t data in the form of t/v vs. v should yield a straight line. By fitting experimental data to the linear relationship between t/v vs. v, the average specific cake resistance and medium resistance can be determined.

2. Initial Period of Filtration. Several recent publications by Koenders and Wakeman[25–27] to analyze cake formation and the interparticle interaction effect on the process. According to these investigators, the initial period of filtration may be described as

$$v = \bar{x}t + \bar{y}t^{3/2} \tag{13}$$

and

$$\bar{x} = p_o/R_m(0) \tag{14}$$

where p_o is the applied pressure, and $R_m(0)$ is the initial medium resistance. In the formulation of Koenders and Wakeman, R_m is considered to be a function of the volume fraction of particles (that is, solidosity).

Similar but not identical expressions of $\bar{y}$ were given in these publications. A general expression of $\bar{y}$, in terms of its dependence on p_o can be written as

$$\bar{y} = b_1 p_o + b_2 p_o^2 \tag{15}$$

b_1 and b_2 may or may not vanish and they are dependent upon the nature of interaction repulsions.

Equation 13 may be arranged to be

$$\frac{v}{t} = \bar{x} + \bar{y}t^{1/2} \tag{16}$$

or a plot of data in the format of v/t vs. $t^{1/2}$ yields a straight line. Based on the value of the intercept of the line, the initial medium resistance can be determined.

3. Analysis of Cake Filtration based on the Solution of the Volume-Averaged Equations of Continuity. More rigorous analysis of cake filtration can be made through the solution of the volume-averaged equations of continuity. The equations describing constant-pressure filtration can be written as[34,35]

$$\frac{\partial \varepsilon_s}{\partial t} = \frac{k^o}{\mu}(\varepsilon_s^o)^{\delta/\beta}\frac{\partial}{\partial x}\left[\varepsilon_s^{-n/\beta}\frac{\partial p_s}{\partial x}\right] + q_{l_m}\frac{\partial \varepsilon_s}{\partial x} \quad 0 < x < L(t) \tag{17}$$

with

$$q_{\ell_m} = -\frac{p_{\ell_m}}{\mu R_m} \tag{18}$$

where x is the distance measured from the medium surface, p_{ℓ_m} is the value of p_ℓ at $x = 0$ (that is, cake/medium interface), q_{ℓ_m} is the instantaneous filtration velocity and is equal to dv/dt.

The cake growth rate, dL/dt is

$$\frac{dL}{dt} = \frac{\varepsilon_s^o}{\varepsilon_s^o - \varepsilon_{s_o}}\left[\frac{k}{\mu}\frac{\partial p_\ell}{\partial x}\right]_{x=L} + q_{\ell_m} \tag{19}$$

and

$$L = 0,\ t = 0 \tag{20}$$

The boundary conditions are

$$-\frac{k}{\mu}\frac{\partial p_\ell}{\partial x} = -\frac{p_\ell}{\mu R_m} \quad x = 0 \tag{21.a}$$

$$p_\ell = p_o,\ p_s = 0 \quad x = L \tag{21.b}$$

The solution of Equations 18–20 with the boundary conditions of Equations 21a and 21b, and the relationships given by Equations 13 and 14 gives the filtration performance results (L vs. t and v vs. t), as well as information about the cake structure and other internal variables as well as these time evolutions.

Effect of operating variables

The results shown in Figure 4 (v vs. t for $CaCO_3$ and Kaolin suspensions) clearly indicate the effect of the medium resistance. As R_m (or number of filter papers used to constitute the medium) increases, there is a corresponding decrease of the filtration rate and, therefore, a decrease of the cumulative filtrate volume. Similarly, the effect of the operating pressure p_o, is shown in Figure 5 which gives the results of v vs. t obtained from experiments carried out under three different p_o, and with different insert plate height. The effect of p_o is clear. The results corresponding to different insert plate heights seemed to overlap and no discernable effect was observed. That the $CaCO_3$ suspension is more filterable than Kaolin suspension shown in this figure is consistent with the C-P cell data of Table 2.

As stated previously, for the purpose of determining the cake thickness history (L vs. t), experiments were conducted by placing the top piston (with an insert plate) at different height. The conditions used for deriving Eq. 8 require uniform suspension flow through the cake formed. The condition is met if there is sufficient distance between the top piston and the cake/suspension interface. However, as the cake thickness approaches to the to piston height, the height effect could become significant. To ascertain this, one should compare the results of v vs. t obtained using different top piston heights over a time period corresponding to the duration of the experiments with the smallest height. This comparison is shown in Figure 6. The results shown in Figure 6 are parts of those of Figure 5 for t up to several hundred seconds, which was approximately the time when the cake thickness reached 10 mm. It becomes rather obvious that the piston height does have an effect; although the nature of the effect is not clear-cut. For example, the cumulative filtrate volume V, with a piston height of 10 mm was the highest at $p_o = 100$ kPa, but the lowest in the other two cases. Furthermore, for $p_o = 800$ kPa, the results obtained with piston height greater than 10 mm seemed to merge together suggesting that as long as the distance between the cake surface

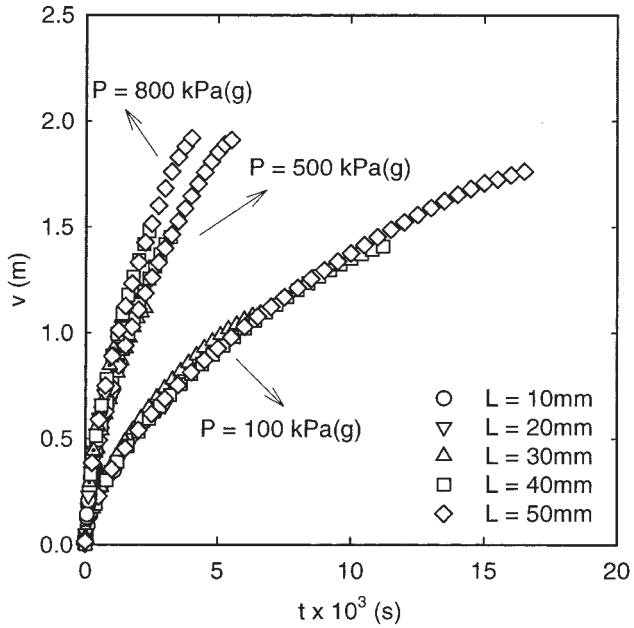

(a) 2% $CaCO_3$ Suspension

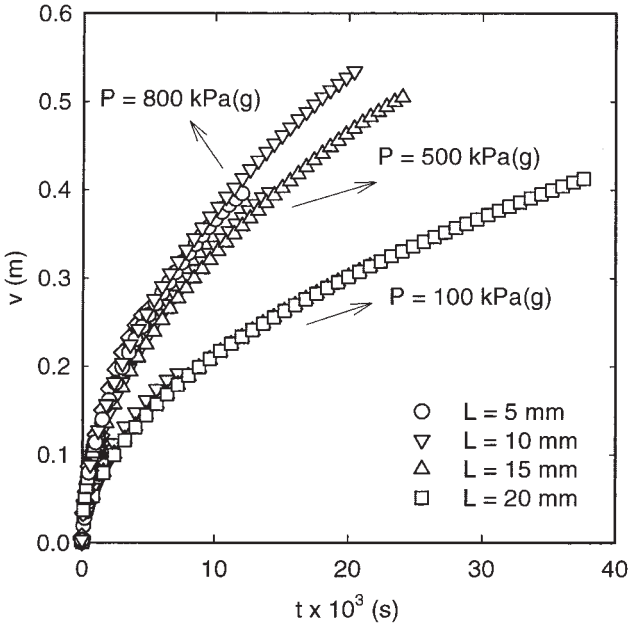

(b) 5% Kaolin Suspension

Figure 5. Effect of operating pressure on filtration performance.

v vs. t obtained from constant-pressure filtration with p_o = 100, 500, 800 kPa, and different preset cake heights with two whatman No. 1 filter paper as medium. (a) 2% $CaCO_3$ suspension, and (b) 5% kaolin suspension.

and the top piston was greater than 10 mm, the effect of the pistons height was negligible.

Parabolic behavior

Equation 8 (or Eq. 12) which is commonly used to describe constant pressure filtration is often referred to as the parabolic law of cake filtration. As this expression was obtained using certain assumptions, questions concerning the general validity of the expression have been raised in the past. Both Tiller et al.[14] and Willis and coworkers[36] discussed the so-called non-parabolic behavior of cake filtration, in their respective studies. Deviation from the parabolic behavior which can be seen from the nonlinearity of the t/v vs. v plot (that is, Equation 12) can be attributed to several factors, including medium clogging because of the penetration of suspended particles into the medium.

A plot of the data shown in Figure 4 in the form of t/v vs. v is given in Figure 7. For a given medium, the linearity of t/v vs. v was observed except for the initial period of filtration (or small values of v) with the nonlinear behavior becoming more pronounced with the increase of the number of filter paper used. Furthermore, the intercept of the t/v vs. v curve appeared to be less than the intercept of the linear segment of the t/v vs. v plot, suggesting the increase of R_m during the course of filtration. However, the nonlinearity of the t/v vs. v plot (or the nonparabolic behavior) cannot be attributed only to the increase in R_m. Equally important is the progressive cake compaction due to the builtup of the cake pressure drop. The non-parabolic behavior diminishes as the cake resistance becomes dominant. The results of Figure 7 are consistent with this argument.

Initial period of filtration

The results obtained by Koenders and Wakeman (namely Eq. 13) suggest that a plot of v/t vs. $t^{1/2}$ for data during the

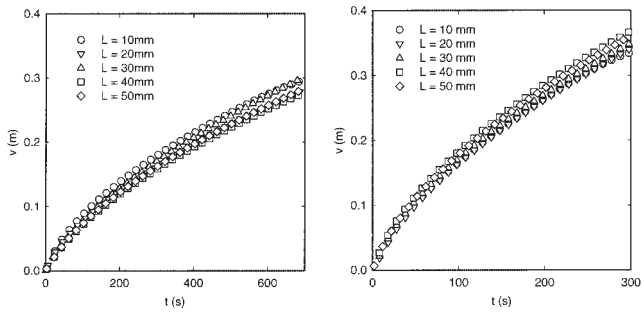

(a) p_o = 100 kPa

(b) p_o = 500 kPa

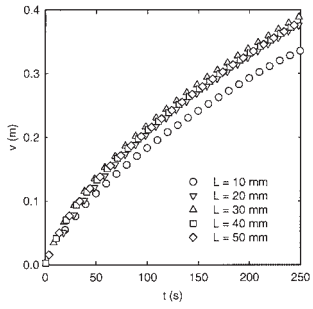

(c) p_o = 800 kPa

Figure 6. Experimental error due to insert plate height.

Data of v vs. t. Constant pressure filtration of 2% $CaCO_3$ with p_o = 100, 500, 800 kPa.

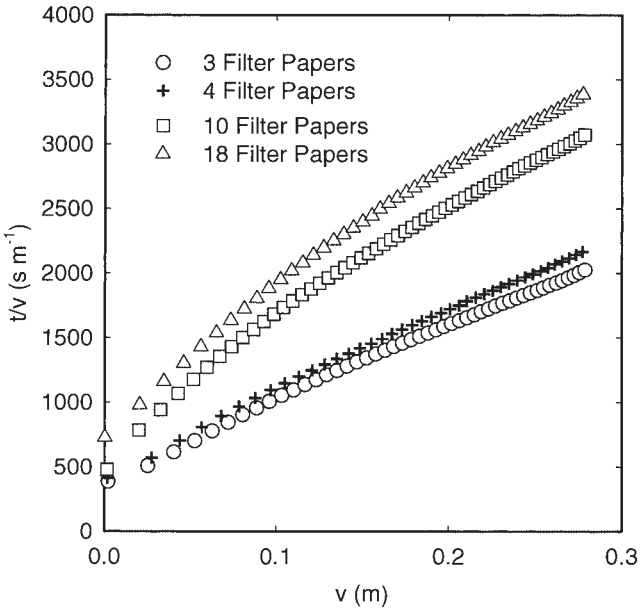

Figure 7. Plot of *t/v* vs. *v*, based on data shown in Figure 4.

Effect of medium resistance on the deviation from linearity of t/v vs. v.

initial period of filtration should yield a straight line. The recent works of Meeten[37] showed that the linearity of v/t vs. $t^{1/2}$ holds for relatively incompressible cakes, but not cakes composed of deformable particles.

The filtration data of $CaCO_3$ suspensions obtained from this study were used to test the validity of Eq. 13. It was assumed that by the initial period, one refers to the period up to the time

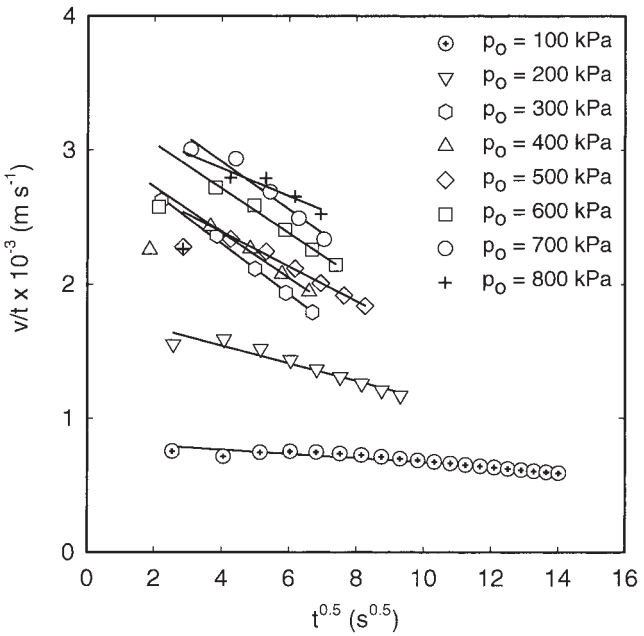

Figure 8. Plot of initial period of filtration data in the format of *v/t* vs. $t^{1/2}$.

Constant pressure filtration of 2% $CaCO_3$ at various p_o.

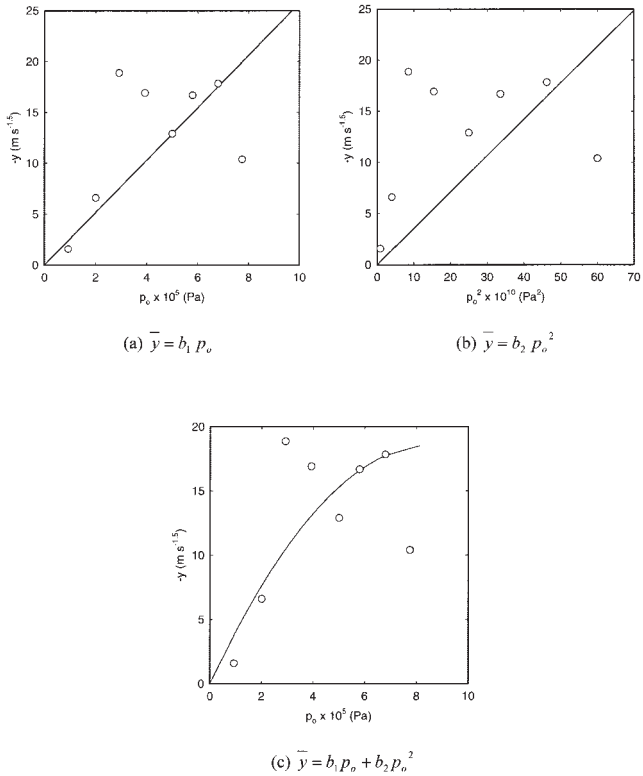

Figure 9. Relationship between $\bar{y}$ and p_o.

Comparisons of Eq. 15. (a) $\bar{y} = b_1 p_o$, (b) $\bar{y} = b_2 p_o^2$, and (c) $p_o = 800$ kPa.

when the pressure drop across the cake reaches half of the applied pressure.[37] For the filtration of 2% $CaCO_3$ suspensions using two filter papers as medium, the initial period ranged from approximately 48 s (for $p_o = 800$ kPa) to 196 s (for $p_o = 100$ kPa). The results are shown in Figure 8.

The results shown in Figure 8 suggest that the linearity of v/t vs. $t^{1/2}$ is at best only approximately observed. As a further assessment, the validity of Eq. 15 was tested. The value of $\bar{y}$ obtained from Figure 8 were fitted according to Eq. 15 with $b_1 = 0$, $b_2 = 0$, or both b_1 and b_2 being nonvanishing. The results are given in Figure 9. It is clear that none of these expressions gives good data fit.

Determination of the specific cake resistance

The conventional method of determining the average specific cake resistance, that is, by fitting filtration data with Eq. 12, was used to obtain (α_{av}). To conform with the conditions used to derive Eq. 12, data of the initial period (as defined earlier) were excluded. From the slope of the linear plot of t/v vs. v, (α_{av}), can be readily obtained if the value of $\bar{m}$ is known. By definition, $\bar{m}$ is given as

$$\bar{m} = \frac{(1 - \bar{\bar{\varepsilon}}_s)\rho + \bar{\bar{\varepsilon}}_s \rho_s}{\bar{\bar{\varepsilon}}_s \rho_s} \tag{22}$$

where $\bar{\bar{\varepsilon}}_s$ is the average cake solidosity. ρ and ρ_s are the filtrate and particle densities, respectively.

The average cake solidosity can be expressed as

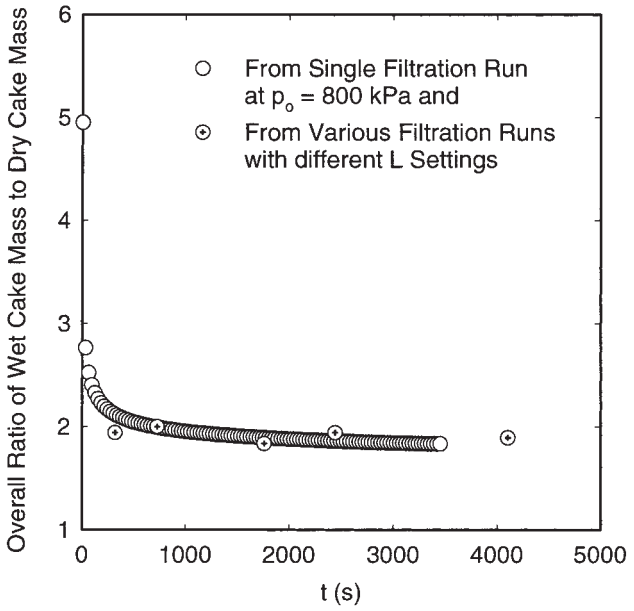

Figure 10. Variation of $\bar{m}$ vs. t; Constant pressure filtration of 2% $CaCO_3$ at p_o = 800 kPa.

$$\bar{\bar{\varepsilon}}_s = \frac{\rho s + \dfrac{\rho s v}{L}}{\rho_s(1-s) + \rho s} \tag{23}$$

Thus, from the data of v vs. t and L vs. t, $\bar{\bar{\varepsilon}}_s$ and $\bar{m}$ can be determined as functions of time. As an example, the results of $\bar{m}$ vs. t of one case (filtration of $CaCO_3$ suspensions at p_o = 800 kPa) are shown in Figure 10. As seen from this figure, except for the very beginning, $\bar{m}$ is essentially constant.

Using constant $\bar{m}$, values of (α_{av}) were determined from filtration data (t/v vs. t) at various values of p_o. If one ignores the medium resistance, p_o can be assumed as the pressure drop across the cake. The results of the four systems ($CaCO_3$, Kaolin, TiO_2 and Kromasil) are presented in Figures 11a–d.*

To compare the results obtained from the constant pressure filtration data with those from the compression-permeability measurements, the relationships between p_ℓ and p_s must be specified first. As pointed out by Tien et al.,[33] a variety of relationships may be assumed. Some of the simpler cases are

$$dp_\ell + dp_s = 0 \qquad (24a) \quad \text{Type (1)}$$

$$(1-\varepsilon_s)dp_\ell + dp_s = 0 \qquad (24b) \quad \text{Type (2)}$$

$$(1-\varepsilon_s)dp_\ell + \varepsilon_s dp_s = 0 \qquad (24c) \quad \text{Type (3)}$$

$$d[(1-\varepsilon_s)p_l] + d[\varepsilon_s p_s] = 0 \qquad (24d) \quad \text{Type (4)}$$

The correspondence between p_ℓ and p_s can be found from the solution of the above equations with $p_s = 0$, at $p_\ell = p_o$ and $p_s = p_{s_m}$ at $p_\ell = 0$.

Accordingly, with the power-law expression of Equation 5, and the values of α^o, n and p_a of Table 3, the relationship of α_{av} vs. p_o can be readily established. These results are also shown in Figure 11a–d. It is clear that for the $CaCO_3$ cakes, the results based on the C-P measurements, and those obtained from the t/v vs. v plot agree well with each other if the $p_\ell - p_s$ relationship is given by Eq. 24b, or Type 2, although the results based on Eq. 24a (or Type 1), differ little from those of Eq. 24b. For Kaolin cakes, Type 3 (that is, Equation 24c) gives the best agreement. For TiO_2 cakes, the data points of (α_{av}) obtained from the constant pressure filtration data have significant scattering, and agree only marginally with the C-P measurement with $p_\ell - p_s$ relationship of Type 2. This is also true for Kromasil cakes.

Determination of medium resistances

The medium resistance can be found from the intercept of the t/v vs. v plot. On the other hand, the medium resistance can also be determined from the value of $(dv/dt)_{t\to o}$ as

$$R_m = \frac{p_o}{\mu\left(\dfrac{dv}{dt}\right)_{t\to o}}$$

$(dv/dt)_{t\to o}$ can be estimated from the results of v vs. t. This was done by first calculating (dv/dt) at various time and by extrapolation, the values at $t \to 0$ was determined. The results of R_m from these two methods are tabulated in Table 6. Also included in the table are the intrinsic values of R_m, namely, R_m

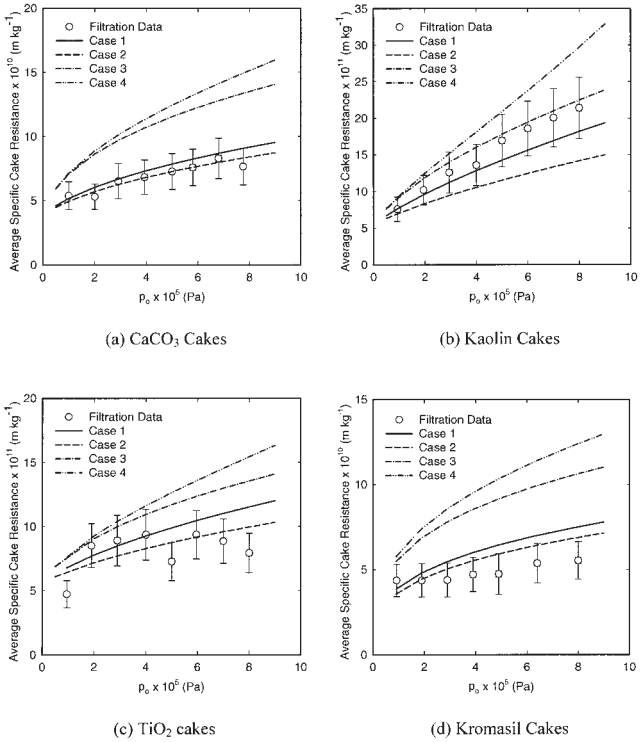

Figure 11. Average specific cake resistance vs. p_o.

Comparisons of C-P measurements results with filtration experimental data: (a) $CaCO_3$ Cakes, (b) Kaolin Cakes, (c) TiO_2 Cakes, and (d) Kromasil Cakes.

* Figures 11a and b were first given by Tien et al.[33]

Table 6. Experimentally Determined Values of Medium Resistance

p_o (Pa) $\times 10^{-5}$	Intrinsic* Medium Resistance (m^{-1}) 1×10^{10}	Medium Resistance, R_m (m^{-1}), 1×10^{11}			
		$CaCO_3$ Suspension		Kaolin Suspension	
		a	b	a	b
1	1.00	1.07	1.15	5.21	2.15
2	1.14	1.25	1.36	8.09	4.52
3	1.11	1.23	1.37	10.1	7.37
4	1.07	1.61	1.86	11.2	11.6
5	1.31	1.98	2.05	10.1	5.75
6	1.50	2.10	2.17	8.91	5.51
7	1.53	2.15	2.34	10.0	8.19
8	1.54	2.26	2.36	9.19	5.72

*Determined by using deionized water
a Determined based on $(dv/dt)_{t\to 0}$
b Determined from t/v vs. v plot

determined by passing deionized water through the medium at various pressures.

The results shown in Table 6 can be summarized as follows: The values of R_m determined from the two methods are rather close; within 10% for the case of $CaCO_3$ and within a factor of two for Kaolin. For both systems, R_m is shown to increase with the increase of p_o. Furthermore, the results differ significantly (by one order of magnitude) from the intrinsic value of R_m, which exhibit only slight dependence on p_o. These findings are consistent with those obtained by Meeten,[37] but differ from the earlier work of Lew and Tiller.[38] The results of Lew and Tiller did not show any simple relationship between R_m and p_o.

The difference between R_m determined from filtration data and its intrinsic value is commonly attributed to medium clogging (for example see Tiller et al.[14]; Lew and Tiller[38]; Lee[39]). Medium clogging may occur in two different ways; interior clogging and surface clogging. For the former, if the suspended particles are not of uniform size, fine particles of sufficiently small sizes may penetrate into the medium and become deposited throughout the medium, thus, causing interior clogging. On the other hand, deposited particles at the cake/medium interface may block or partially block various pore entrances of the medium. In either case, the effective medium resistance is increased.

Interior clogging was considered the major cause for the increase in R_m by Lee.[39] This may indeed be correct if fine particles (those with sizes considerably less than the pore openings of the medium) present in the suspension are significant. From the size distributions of the powders used in Meeten's work and this study, this condition was not met. On the other hand, the extent of surface clogging of a medium is determined largely by the compaction of the deposited particle, which, in turn, is dependent upon the local compressive stress of the cake phase. For constant pressure filtration, the compressive stress at the cake/medium interface increase with time and approaches to the value corresponding to $p_\ell = p_o$. The experimentally determined value of R_m, as an approximation, can, therefore, be considered as a function of p_o if surface clogging is the dominant clogging mechanism. The results given in Table 6 are consistent with this speculation.

If one considers medium clogging occurs at membrane surface, and the extent of clogging is determined by the compressive stress at the cake/medium interface using a constant R_m in predicting filtration performance is, at best, an approximation. The error introduced by this approximation can be seen from a sample calculation based on Eq. 8. Assuming that

$$\frac{\rho s}{2(1-\bar{m}s)} = 10\ \mathrm{kg\cdot m^{-3}},\ \mu = 10^{-3}\ \mathrm{Pa\cdot s^{-1}},\ \alpha_{av} = 5 \times 10^{10}\ \mathrm{m\cdot kg^{-1}}$$

and $R_m = 10^{10}$, 10^{11}, $2 \times 10^{11} m^{-1}$ (typical values for the case of $CaCO_3$), the results obtained (v vs. t) are given in Table 7. It is clear that for filtration calculations, the intrinsic value R_m should not be used. On the other hand, R_m determined from filtration data can be used for calculations as long as the applied pressure is of the same order of magnitude of the pressure with which the experimental data were obtained.

Comparisons with prediction based on the solution of the volume-averaged equations of continuity

In recent years, a number of studies on the prediction of cake filtration performance based on the multiphase flow theory have appeared in the literature.[34–35,40–44] However, validation of predictions was made only in a limited way because of lack of appropriate experimental data. With the results obtained from the present work, a more complete assessment of these predictions becomes possible. Furthermore, through the comparisons, the effect of the $p_l - p_s$ effect was assessed.

The experimental data used in comparison includes the cumulative filtrate volume vs. time results for the four kinds of suspensions and the cake thickness histories of the filtration of $CaCO_3$ and Kaolin suspensions. The information required for predicting cake filtration performance for a specified set of the

Table 7. Sample Calculations of Filtration Performance using Different Values of R_m Conditions Assumed $p_o = 800$ kPa; $(\alpha_{av}) = 5 \times 10^{10}$ m kg^{-1}; $s = 0.02$; $\rho = 10^3$ kg m^{-3}; $\mu = 10^{-3}$ Pa-s

Time (s)	R_m 1×10^{10} m^{-1}	v (m^3/m^2)	
		1×10^{11} m^{-1}	2×10^{11} m^{-1}
100	0.3901	0.3123	0.2472
200	0.5558	0.4775	0.4000
400	0.7901	0.7063	0.6248
1,000	1.253	1.1689	1.0806

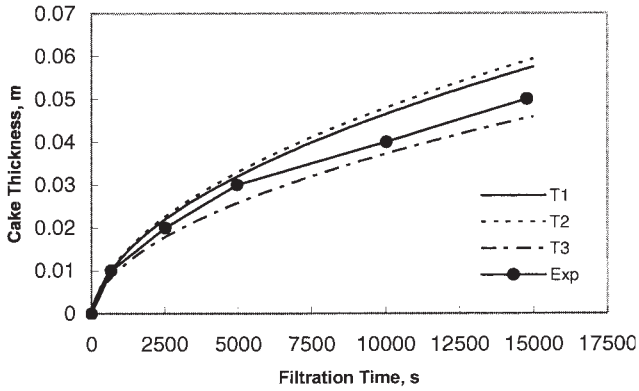

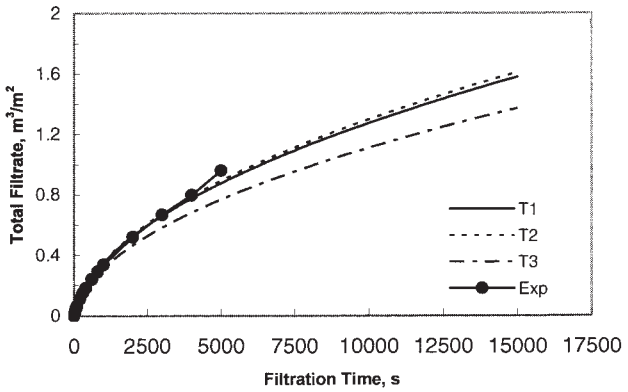

(a) p_o = 100 kPa

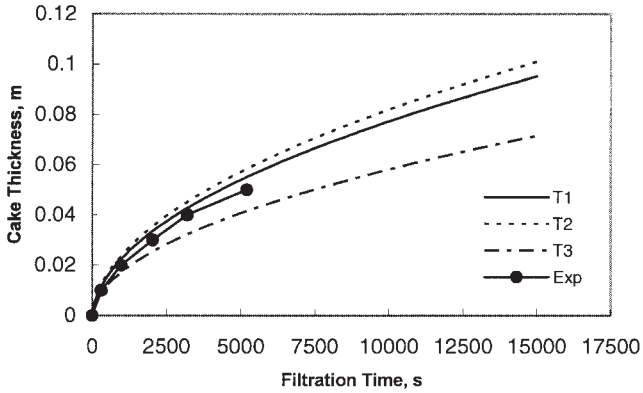

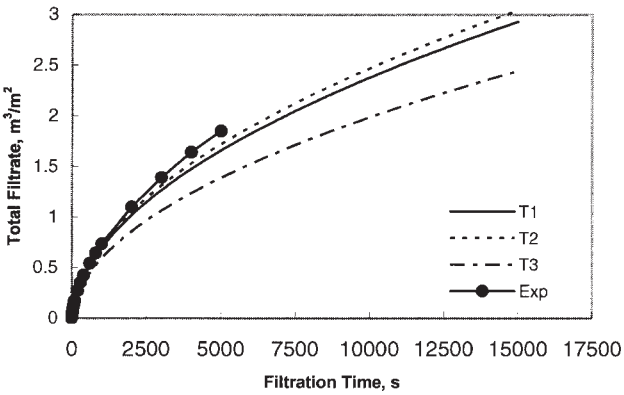

(b) p_o = 500 kPa

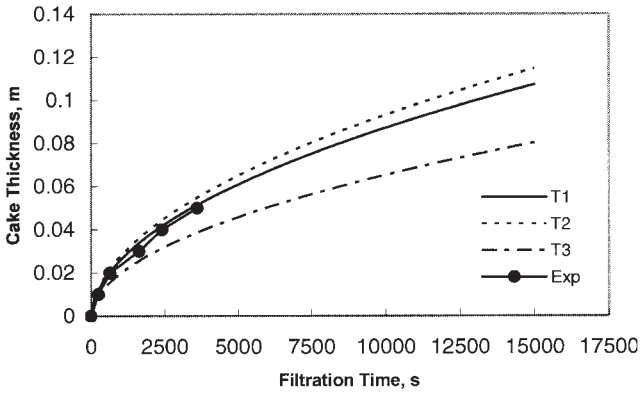

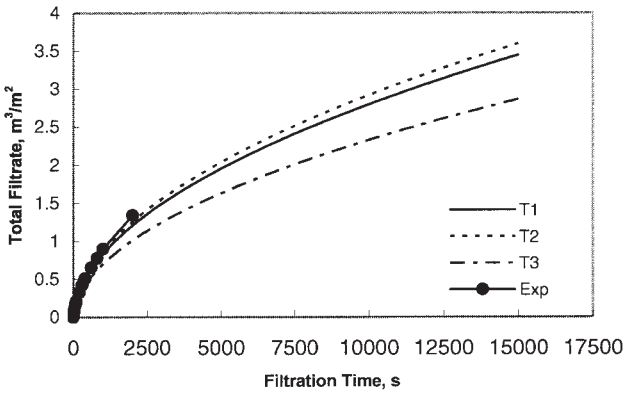

(c) p_o = 800 kPa.

Figure 12. Comparisons of predictions with experiments.

Constant pressure filtration 2% $CaCO_3$ suspensions. (a) p_o = 100 kPa, (b) p_o = 500 kPa, and (c) p_o = 800 kPa.

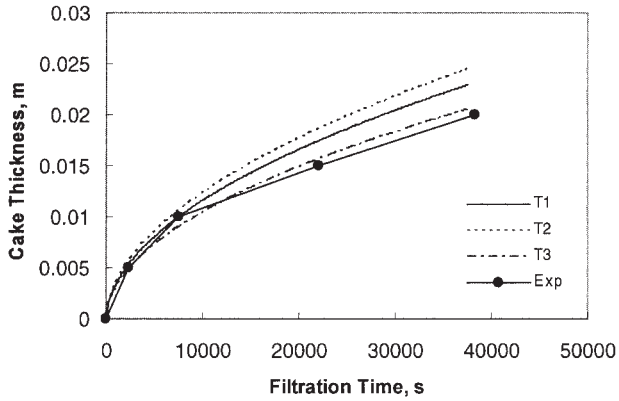

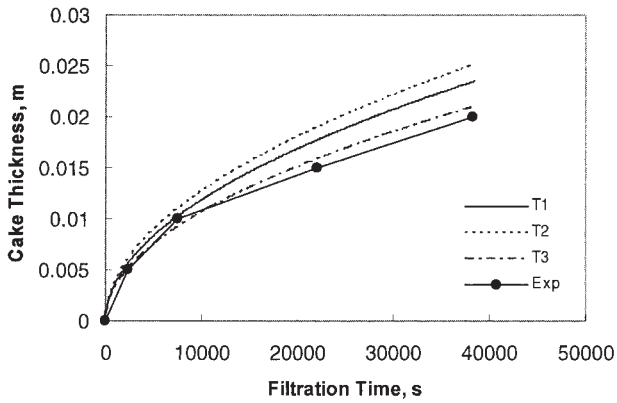

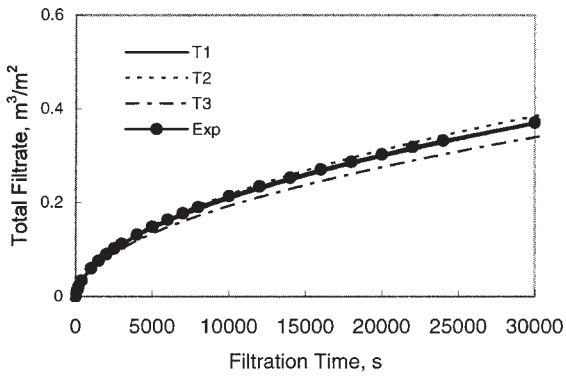

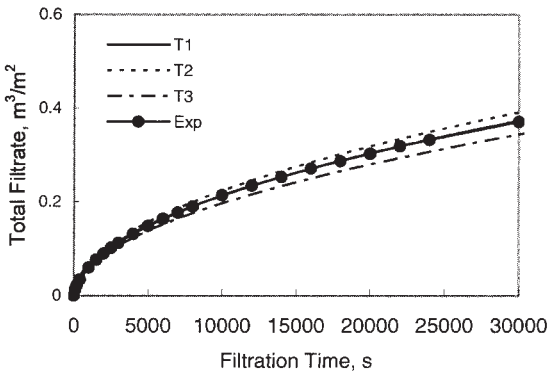

(a) p_o = 100 kPa, $R_m = 2.15\times10^{11}$ m^{-1}

(b) p_o = 100 kPa, $R_m = 5.21\times10^{11}$ m^{-1}

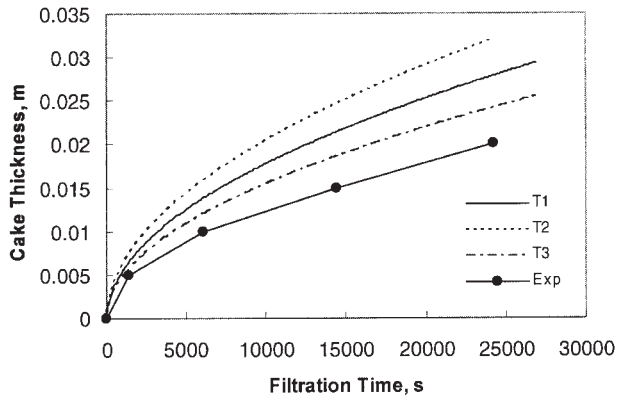

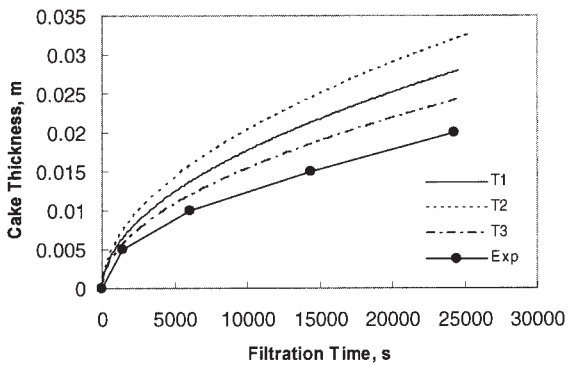

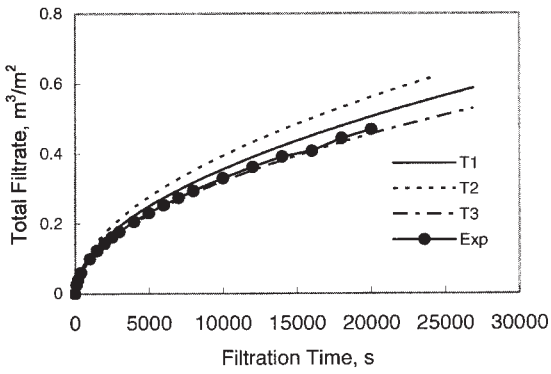

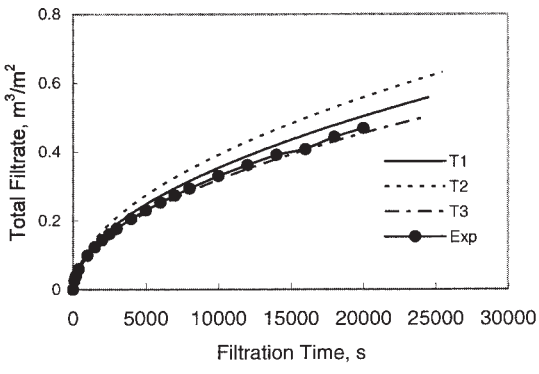

(c) p_o = 500 kPa, $R_m = 6.9\times10^{11}$ m^{-1}

(d) p_o = 500 kPa $R_m = 9.5 \times 10^{11}$ m^{-1}.

Figure 13. Comparisons of predictions with experiments.

Constant pressure filtration 5% Kaolin suspensions; (a) $p_o = 100$ kPa, $R_m = 2.15 \times 10^{11}$ m^{-1}, (b) $p_o = 100$ kPa, $R_m = 5.21 \times 10^{11}$ m^{-1}, (c) $p_o = 500$ kPa, $R_m = 6.9 \times 10^{11}$ m^{-1}, and (d) $p_o = 500$ kPa, $R_m = 9.5 \times 10^{11}$ m^{-1}.

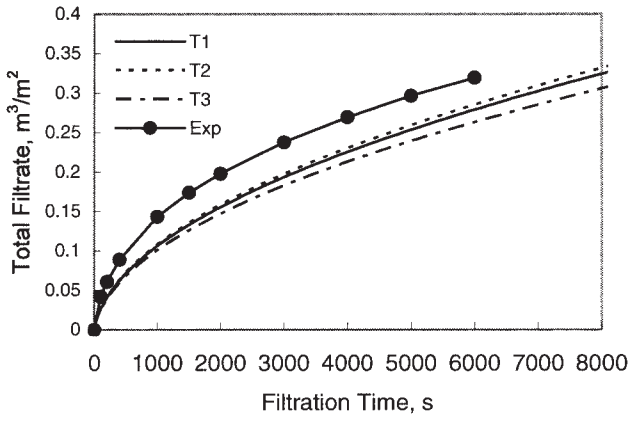

(a) p_o = 100 kPa, $R_m = 2.15\times10^{11}$ m^{-1}

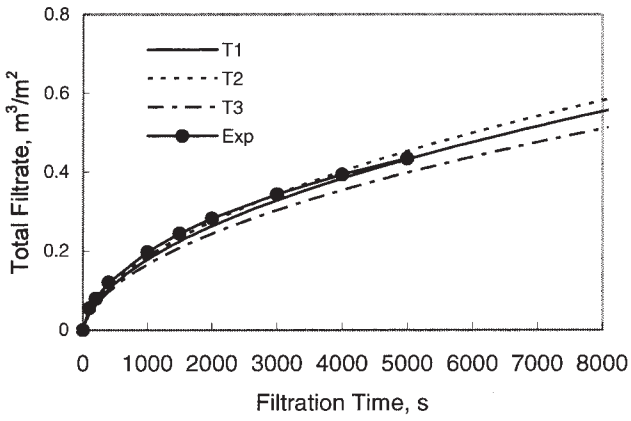

(b) p_o = 400 kPa, $R_m = 6.9\times10^{11}$ m^{-1}

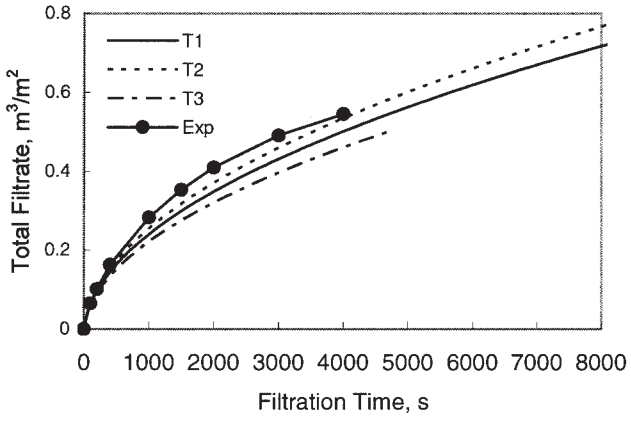

(c) p_o = 800 kPa, R_m = 6.9 x 10^{11} m^{-1}.

Figure 14. Comparisons of predictions with experiments.

Constant pressure filtration, 2% TiO_2 suspensions; (a) p_o = 100 kPa, $R_m = 2.15 \times 10^{11}$ m^{-1}, (b) p_o = 400 kPa, $R_m = 6.9 \times 10^{11}$ m^{-1}, and (c) p_o = 800 kPa, $R_m = 6.9 \times 10^{11}$ m^{-1}.

operating variables include the values of the parameters of the constitutive relationships of the relevant systems and the values of the medium resistance. The parameter values are those given in Table 3. The medium resistance values for the $CaCO_3$ and Kaolin case are listed in Table 6. As explained previously, two different methods were used in the evaluation of R_m. For the case of $CaCO_3$ suspensions, the values obtained from the two methods are very similar and their averages were used. For Kaolin suspensions, the R_m values obtained showed significant scattering. It was decided that for the case of p_o = 100 kPa, both of these two values (corresponding to methods a and b) were used. For p_o = 500 and 800 kPa, because of the scattering of data, the two averages of R_m at p_o = 500, 600, 700 and 800 kPa were used. By using two different values of R_m for the same prediction, the effect of R_m was also examined.

R_m values for the cases of Kromasil and TiO_2 were not determined in this work. Based on the fact that R_m depends, to a degree, on the extent of surface clogging due to cake compaction as argued previously, as the compressibility of TiO_2 cakes is similar to Kaolin cakes (see Table 3), the R_m value used for predicting Kaolin suspension filtration were also used for the case of TiO_2. Using the same argument, predictions of the filtration of Kromasil suspension were made using the R_m values of the $CaCO_3$ case according to Method (a).

The comparison results shown in Figures 12–15 may be summarized as follows:

(a) $CaCO_3$ Suspensions. Comparisons of the filtration results of v vs. t and L vs. t for p_o = 100, 500, and 800 kPa are shown in Figure 12a, 12b and 12c. For p_o = 100 kPa, experimental data of v vs. t agree well with prediction using either Type 1 or Type 2 $p_l - p_s$ relationship with Type 2 relationship yielding slightly better agreement. On the other hand, better agreement (especially initially) was predicted using Type 1 relationship was found for the results of L vs. t. For p_o = 500 kPa, the experimental results of L vs. t were shown to agree well with prediction using either Type 1 or Type 2 relationship. The results of L vs. t were lower than either prediction although they agree better with prediction using Type 1 $p_l - p_s$ relationship. The same trend was observed for the results obtained at p_o = 800 kPa.

Previously, the average specific cake resistances obtained from filtration results (through t/v vs. v plot) were compared with those based on C-P cell measurements using different $p_l - p_s$ relationship. As shown in Figure 11, one may conclude that either Type 1 or Type 2 relationship may be applied to characterize the $p_l - p_s$ relationship for $CaCO_3$ cakes. The results shown in Figure 12 are consistent with the earlier conclusions.

(b) Kaolin Suspensions. The comparisons are shown in Figure 13. As stated before, two different values of R_m were

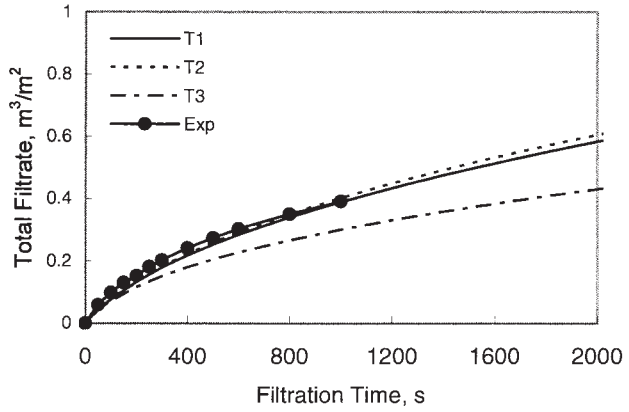

(a) $p_o = 100$ kPa

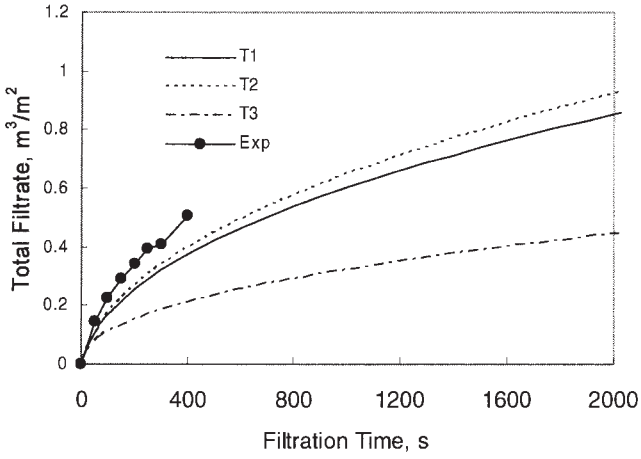

(b) $p_o = 400$ kPa

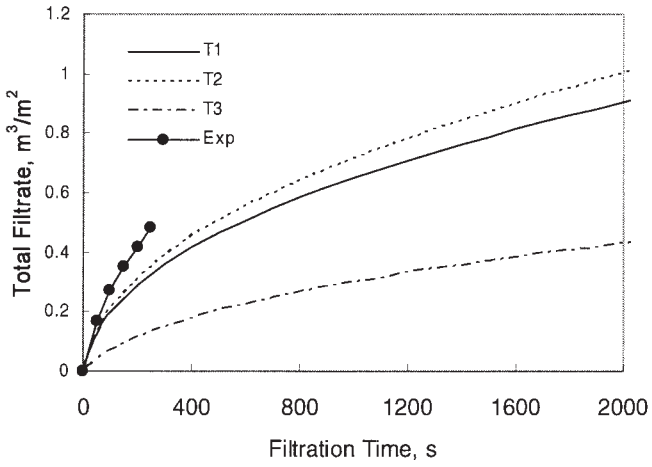

(c) p_o =800 kPa

Figure 15. Comparisons of predictions with experiments.

Constant pressure filtration. 2% Kromasil suspensions; (a) $p_o = 100$ kPa, (b) $p_o = 400$ kPa, and (c) $p_o = 800$ kPa.

used for each prediction. For the prediction of v vs. t, at $p_o = 100$ kPa, the effect of using different R_m was slight and the prediction based on Type 1 $p_l - p_s$ relationship agree well with experiments. The effect of using different R_m in the prediction of cake thickness history was also insignificant. However, the L vs. t data was found to agree with predictions using Type 3 $p_l - p_s$ relationship. For the results obtained at $p_o = 500$ kPa, the L vs. t data agree well with predictions using Type 3 $p_l - p_s$ relationship. The effect of using different R_m was also slight. All predictions were found to overestimate the cake thickness although the predictions based on Type 3 $p_l - p_s$ relationship gave the least deviation.

Comparisons of the specific cake resistance (shown in Figure 11b) indicate that at lower pressure ($p_o \leq 200$ kPa), Type 1 $p_l - p_s$ relationship gives the best agreement, but at high p_o, better agreement with Type 3 relationship was observed. There appears to be a degree of corroboration between the results of Figure 11 and those of Figure 13.

(c) TiO_2 Suspensions. At $p_o = 100$ kPa, all predictions underestimate the v vs. t results although predictions based on Type 2 $p_l - p_s$ relationship give the least differences. The results obtained at $p_o = 400$ kPa agreed best with predictions based on Type 1 $p_l - p_s$ relationship and predictions, based on Type 2 relationship give the best comparisons with data obtained at $p_o = 800$ kPa.

The results shown in Figure 11c show that the specific cake resistance obtained from the t/v vs. v plot compared rather poorly with those based on the C-P cell measurements. Relatively speaking, the result obtained from the t/v vs. v plot with $p_o \leq 400$ kPa agreed better with Type 1 relationship, but Type 2 relationship seemed to give better results for $p_o > 400$ kPa.

(d) Kromasil Suspension. At $p_o = 400$ kPa, either Type 1 or Type 2 $p_l - p_s$ relationship gave agreement with experimental data of v vs. t. At higher pressures, all predictions underestimate although Type 2 relationship gives the least deviation. These observations are consistent with what is shown in Figure 11d.

The agreement between prediction and experiments vary among the four cases. However, they corroborate well with the specific cake resistance comparisons of Figure 11a–d. For example, the underestimation of v in the case of Kromasil (for $p_o = 400$, 800 kPa) results directly from an overestimation of the specific resistance as demonstrated in Figure 11d. And the good agreement shown in Figure 12a–c can be linked directly to the good agreement of Figure 11a. A prima facie case on the importance of identifying the proper $p_l - p_s$ relationship used

in analyzing cake filtration may therefore be made based on these comparisons.

Conclusions

Based on the results obtained in this study as presented earlier, the following conclusions can be made.

1. The results of ε_s vs. p_s, k vs. p_s and α vs. p_s obtained from the multifunction test cell can be fitted by the power-law expressions.

2. Parabolic behavior which is commonly assumed valid for constant pressure filtration was observed in all cases except initially. The extent of nonlinearity increase as the medium resistance increases.

3. Limited agreement between the initial period of filtration data and the analysis of Koenders and Wakeman was obtained.

4. With proper $p_l - p_s$ relationship, the average specific cake resistances determined based on constant-pressure filtration data using the t/v vs. v plot can be corroborated with those based on the C-P cell measurement.

5. The medium resistance is shown to be time-dependent, and its increase with time can be attributed to surface clogging.

6. Predictions of filtration performance, based on the solution of the volume-averaged equations of continuity agree well with experiments if the appropriate $p_l - p_s$ relationship is used in the prediction.

Acknowledgment

The authors would like to thank the National Science & Technology Board (NSTB) for funding this research work, as well as Dr. Bai of National University of Singapore.

Notation

A = cross sectional area of test cell, m^2
b_1, b_2 = coefficients of Eq. 15
F_A = force applied, N
F_t = force transmitted, N
f' = defined by Eq. 10
k = cake permeability, m^2
k^o = value of k at zero stress state, m^2
L = cake thickness, m
m = mass of particles, kg
$\bar{m}$ = wet to dry cake mass ratio
n = exponent of Eq. 5
p_a = parameter of Eqs. 3, 4 and 5, Pa
p_ℓ = liquid pressure, Pa
p_o = applied pressure, Pa
p_s = cake compression stress, Pa
p_{s_m} = value of p_s at cake/medium interface, Pa
Q = volumetric flow rate, $m^3\ s^{-1}$
q_s = liquid flow rate, ms^{-1}
q_{ℓ_m} = instantaneous filtration rate, ms^{-1}
R_m = medium resistance, m^{-1}
s = particle mass fraction
t = time, s
V = cumulative filtrate volume, m^3
v = cumulative filtration volume per unit medium area, m^3/m^2
x = distance measured away from medium, m
$\bar{x}$, $\bar{y}$ = coefficients of Eq. 13

Greek letters

α = specific cake resistance, m kg^{-1}
α^o = value of α at the zero stress state, m kg^{-1}
α_{av} = average specific cake resistance, m kg^{-1}
β = exponent of Eq. 3
ε_s = cake solidosity
ε_s^o = value of ε_s at zero stress state
ε_{s_o} = particle volume fraction of suspension
Δp = pressure drop, Pa
η = exponent of Eq. 4
μ = filtrate viscosity, Pa-s
ρ_s = particle density, kg m^{-3}

Literature Cited

1. Ruth BF, Montillon GH, Montonna RE. Studies in filtration, I. Critical analysis of filtration theory. *Ind Eng Chem.* 1933;25:76–82.
2. Ruth BF, Montillon GH, Montonna RE. Studies in filtration, II. Fundamental axiom of constant pressure filtration. *Ind Eng Chem.* 1933; 25:153–161.
3. Grace HP. Resistance and compressibility of filter cakes, Part 1. *Chem Eng Prog.* 1953;49:303–318.
4. Grace HP. Resistance and compressibility of filter cakes, Part 2: Under conditions of pressure filtration. *Chem Eng Prog.* 1953;44:427–436.
5. Tiller FM. The role for porosity in filtration I: Numerical methods. *Chem Eng Prog.* 1953;49:467–479.
6. Tiller FM. The role for porosity in filtration II: Analytical equations for constant rate filtration. *Chem Eng Prog.* 1953;51:282–290.
7. Tiller FM. The role for porosity in filtration III: Variable pressure—Variable rate filtration. *AIChE J.* 1958;4:170–174.
8. Tiller FM. The role for porosity in filtration IV: Constant pressure filtration. *AIChE J.* 1960;6:565–601.
9. Tiller FM. The role for porosity in filtration V: Porosity variation in filter cakes. *AIChE J.* 1962;8:445–449.
10. Tiller FM. The role for porosity in filtration VI: New definition of filtration resistance. *AIChE J.* 1964;10:61–67.
11. Tiller FM. The role for porosity in filtration VII: Effects of sidewall friction in compression-permeability cells. *AIChE J.* 1972;18:13–20.
12. Tiller FM. The role for porosity in filtration VIII: Cake nonuniformity in compression-permeability cells. *AIChE J.* 1972;18:569–572.
13. Tiller FM. The role for porosity in filtration IX: Shine effect with highly compressible materials. *AIChE J.* 1973;19:1266–1269.
14. Tiller FM, Chow R, Weber WH, David O. Clogging phenomena in liquefied coal. *Chem Eng Prog.* 1981, Dec;77:61–68.
15. Tiller FM, Shirato M, Alciatore A. Filtration in the Chemical Process Industry. In: Matteson MJ, Orr C. *Filtration: Principles and Practices,* 2nd ed. New York: Marcel Dekker; 1987:361–474.
16. Tiller FM, Yeh CS. The role of porosity in filtration X: Deposition of compressible cakes on external surfaces. *AIChE J.* 1985;31:1241–1248.
17. Tiller FM, Yeh CS. The role of porosity in filtration XI: Filtration followed by expression at high pressure. *AIChE J.* 1987;33:1241–1256.
18. Tiller FM, Lu R, Kwon KW, Lee DJ. Variable flow rate in compactible filter cakes. *Water Research.* 1999;33:15–22.
19. Shirato M, Okamura S. Behaviours of gaisome-clay slurries at constant pressure filtration. *Kagaku Kagaku.* 1956;20:678–684.
20. Shirato M, Aragaki T, Mori R, Sawamoto K. Predictions of constant pressure and constant rate filtration based on approximate correction for side wall friction in compression-permeability cell data. *J Chem Eng.* (Japan). 1968;1:86–90.
21. Shirato M, Sambuichi M, Kato H, Aragaki T. Internal flow mechanism in filter cakes. *AIChE J.* 1969;15:405–409.
22. Shirato M, Aragaki T. The relations between hydraulic and compression pressures in non uni-dimensional filter cake. *Kagaku Kagaku.* 1969;33:205–207.
23. Shirato M, Aragaki T, Mori R, Imai K. Study of variable pressure variable rate filtration. *Kagaku Kogaku.* 1969;33:576–581.
24. Shirato M, Aragaki T, Ichimura K, Ootsuji N. Porosity variation in filter cake under constant pressure filtration. *J Chem Eng (Japan).* 1971;4:172–177.
25. Koenders MA, Wakeman RJ. The initial stages of compact formation from suspensions by filtration. *Chem Eng Sci.* 1996;51:3897–3906.
26. Koenders MA, Wakeman RJ. Filter cake formation from structured suspension. *Trans I Chem E.* 1997;75, Part A:309–320.
27. Koenders MA, Wakeman RJ. Initial deposition of interacting particles by filtration of dilute suspensions. *AIChE J.* 1997;43:946–958.
28. Murase T, Iritami E, Cho JH, Nakomori S, Shirato M. Determination

of filtration characteristics due to sudden reduction in filtration area of filtration cake surface. *J Chem Eng.* (Japan). 1987;20:246–251.
29. Tan RBH, He D, Tien C. Multifunction Test Cell for Filtration Studies. Singapore Patent No. 9804082-7. 1998.
30. Teoh SK, Tan RBH, He D, Tien C. A multifunction test cell for cake filtration studies. *Trans Filtration Soc.* 2001;1:81–90.
31. Teoh SK. Studies in filter cake characterization and modeling. National University of Singapore. 2003. PhD. Thesis.
32. Lu WH, Huang YP, Hwang K. Stress distribution in a confined wet cake in the compression-permeability cell and its applications. *Powder Tech.* 1998;97:12–65.
33. Tien C, Teoh SK, Tan RBH. Cake filtration analysis—The effect of the relationship between pore liquid pressure and cake compressive stress. *Chem Eng Sci.* 2001;56:5361–5369.
34. Tien C, Bai R. Assessment of the conventional cake filtration theory. *Chem Eng Sci.* 2003;58:1323–1336.
35. Tien C, Bai R. Numerical Analysis of Cake Filtration. *9th World Filtration Congress,* Paper 214-5. April 2004; New Orleans, LA.
36. Willis MS, Collins RM, Bridges WG. Complete analysis of non-parabolic filtration behavior. *Chem Eng Res Des.* 1983;61:96–109.
37. Meeten GH. Septum and filtration properties of rigid and deformable particle suspensions. *Chem Eng Sci.* 2000;55:1755–1967.
38. Lew WF, Tiller FM. Experimental study of the mechanism of constant pressure filtration. *Sep Sci Tech.* 1983;18:1351–1369.
39. Lee DJ. Filter medium clogging during cake filtration. *AIChE J.* 1997;42:273–276.
40. Tosun I. Formulation of cake filtration. *Chem Eng Sci.* 1986;41:2563–2568.
41. Stamatakis K, Tien C. Cake formation and growth in cake filtration. *Chem Eng Sci.* 1991;46:1917–1933.
42. Landman KA, White LR, Eberl M. Pressure filtration of flocculated suspensions. *AIChE J.* 1995;41:1687–1700.
43. Tien C, Bai R, Ramarao BV. Analysis of cake growth in cake filtration: Effect of fine particle retention. *AIChE J.* 1997;43:33–44.
44. Burger R, Concha F, Karlsen KH. Phenomenological model of filtration processes: 1. Cake formation and expression. *Chem Eng Sci.* 2001;56:4337–4553.

Manuscript received Aug. 6, 2005, and final revision received Jun. 28, 2006.